Suppression of Human Glioma Xenografts with Second-Generation IL13R-Specific Chimeric Antigen Receptor–Modified T Cells

Seogkyoung Kong[1], Sadhak Sengupta[1], Betty Tyler[4], Anthony J. Bais[2], Qiangzhong Ma[2], Saryn Doucette[3], Jinyuan Zhou[5], Ayguen Sahin[6], Bob S. Carter[6], Henry Brem[4], Richard P. Junghans[2], and Prakash Sampath[1]

Abstract

Purpose: Glioblastoma multiforme (GBM) remains highly incurable, with frequent recurrences after standard therapies of maximal surgical resection, radiation, and chemotherapy. To address the need for new treatments, we have undertaken a chimeric antigen receptor (CAR) "designer T cell" (dTc) immunotherapeutic strategy by exploiting interleukin (IL)13 receptor α-2 (IL13Rα2) as a GBM-selective target.

Experimental Design: We tested a second-generation IL13 "zetakine" CAR composed of a mutated IL13 extracellular domain linked to intracellular signaling elements of the CD28 costimulatory molecule and CD3ζ. The aim of the mutation (IL13.E13K.R109K) was to enhance selectivity of the CAR for recognition and killing of IL13Rα2+ GBMs while sparing normal cells bearing the composite IL13Rα1/IL4Rα receptor.

Results: Our aim was partially realized with improved recognition of tumor and reduced but persisting activity against normal tissue IL13Rα1+ cells by the IL13.E13K.R109K CAR. We show that these IL13 dTcs were efficient in killing IL13Rα2+ glioma cell targets with abundant secretion of cytokines IL2 and IFNγ, and they displayed enhanced tumor-induced expansion versus control unmodified T cells *in vitro*. In an *in vivo* test with a human glioma xenograft model, single intracranial injections of IL13 dTc into tumor sites resulted in marked increases in animal survivals.

Conclusions: These data raise the possibility of immune targeting of diffusely invasive GBM cells either via dTc infusion into resection cavities to prevent GBM recurrence or via direct stereotactic injection of dTcs to suppress inoperable or recurrent tumors. Systemic administration of these IL13 dTc could be complicated by reaction against normal tissues expressing IL13Ra1. *Clin Cancer Res; 18(21); 5949–60. ©2012 AACR.*

Introduction

Glioblastoma multiforme (GBM) is the most common and lethal of adult brain cancers. GBM is currently treated with surgical resection, radiation, and chemotherapy (1). Despite recent advances with multimodality interventions, the majority of patients survive less than 20 months due to tumor recurrence (2, 3). Therefore, new therapies are needed to prevent such recurrence and improve patient survivals.

Here, we report a strategy of genetic modification of T cells ("designer T cells") to redirect their killing specificity against GBM cells while leaving normal brain unharmed.

T cells can be modified using viral or plasmid vectors to express a chimeric antigen receptor (CAR), providing a large population of patient-derived designer T cells (dTc) with the power to recognize tumor-specific antigens (4). The CAR is a single molecule comprising an extracellular tumor antigen–binding domain, a transmembrane domain, and cytoplasmic signaling domains for T-cell activation. The resulting modified T cells are redirected by the neospecificity of the CAR to attack tumors expressing the surface antigen. T-cell recognition is mediated in an MHC-independent fashion, resulting in a more broadly applicable therapy that also avoids mechanisms of tumor escape via downregulation of MHC-I that has been reported in glioblastomas (5). Direct, locoregional delivery of GBM-specific T cells into the surgical bed at the time of tumor resection has the potential to eradicate residual, invasive glioblastoma cells and prevent tumor recurrence. Glioma-specific dTc therapy is being actively pursued in both preclinical studies and clinical trials (6–8).

Interleukin (IL) 13 receptor α-2 (IL13Rα2) is a GBM-associated protein that is overexpressed on virtually all GBM

Authors' Affiliations: [1]Brain Tumor Lab, Department of Neurosurgery, [2]Biotherapeutics Development Lab, Department of Medicine, [3]Department of Pathology, Boston University School of Medicine, Roger Williams Medical Center, Providence, Rhode Island; [4]Hunterian Neurosurgical Research Laboratory, Department of Neurosurgery, [5]Department of Radiology, Johns Hopkins University School of Medicine, Baltimore, Maryland; and [6]Department of Neurosurgery, Massachusetts General Hospital, Boston, Massachusetts

Corresponding Author: Richard P. Junghans, Department of Medicine, Boston University School of Medicine, Roger Williams Medical Center, 825 Chalkstone Avenue, NC 143, Providence, RI 02908. Phone: 401-456-2507; Fax: 401-456-4812; E-mail: rpj@bu.edu

Translational Relevance

Targeted immunotherapy has received a great deal of interest in recent years with the aim to apply a cytotoxic agent that preferentially targets tumor cells, without damage to the surrounding brain tissue. Chimeric antigen receptors (CAR) that are fusion products of an antibody or ligand-binding domain with the zeta signaling chain of the T-cell receptor (TCR) is a promising strategy for targeted immunotherapy of malignant tumors. Resulting "designer T cells" (dTc) are redirected by the neospecificity to attack tumors expressing the surface antigen recognized by the CARs. This strategy is designed to bypass a major drawback of cancer immunotherapy, which has been hampered by the fact that most "tumor antigens" are normal self-proteins to which the patient is already tolerized. Interleukin (IL)13 receptor α-2 (IL13Rα2) was selected as a target antigen because it is highly overexpressed in most gliomas. This same receptor is minimally or not expressed in normal brain tissue making it a suitable candidate for targeting with immunotherapy. The successful application of such dTcs in animal models is encouraging for their translation into human clinical settings for treatment of resection cavity or recurrent gliomas.

tumors but minimally or not at all in normal brain tissues (9,10). As such, IL13Rα2 was considered suitable as a GBM-selective antigen, a rationale that has supported the targeting of GBM within the central nervous system (CNS) in the clinical development of IL13 immunotoxin molecules (11) and IL13 designer T cells (6).

The GBM-associated IL13Rα2 receptor has a moderate to high affinity for IL13 ($K_d = 0.25–1.2$ nmol/L; ref. 12). The widespread, normal tissue-associated receptor, IL13Rα1, is structurally distinct, with an approximate 10-fold lower affinity for IL13 ($K_d = 2–30$ nmol/L; refs. 13–15). In the presence of IL4R, however, IL13Rα1 will form a ternary complex with IL13 (IL13Rα1/IL13/IL4Rα) that is of very high affinity ($K_d = 0.1–0.4$ nmol/L; refs. 13, 14). In context with IL4Rα, IL13Rα1 will bind IL4 as well as IL13, but as an isolated receptor, IL13Rα1 will bind only IL13. IL13Rα2 is always an isolated receptor and only binds IL13.

In this study, we adapt a previously described "zeta-kine" approach (6) to express an IL13 CAR on dTcs to provide recognition and targeting of IL13Rα2 on GBM tumors. Previous studies have shown that substitutions at different sites in IL13 could either enhance IL13 binding to IL13Rα2 or block IL13 binding to IL4Rα that generates the high-affinity IL13Rα1/IL4Rα receptor (15–17). Using this information, we created a novel mutant (IL13.E13K. R109K) to improve the selectivity for IL13Rα2 on GBM versus IL13Rα1/IL4Rα on normal tissues. Furthermore, we incorporated a CD28 signaling domain into the CAR to provide signal 2 costimulation with CD3ζ signal 1 for improved dTc survival and function. Finally, we created

monomeric and dimeric forms of the CAR to test hypotheses of CAR receptor binding and activation. *In vitro* testing and an *in vivo* model for intracranial locoregional administration provide data that are encouraging for ultimate human application.

Materials and Methods

Cell lines and cultures

The human glioma cell line U251 was obtained from H. Brem (Johns Hopkins, Baltimore, MD). Thp-1, human umbilical vein endothelial cell (HUVEC), 293, and Daudi cell lines were obtained from American Type Culture Collection (ATCC).

Construction of CAR gene in expression vector

cDNA clone encoding full-length hIL13 was obtained from Open Biosystems (GenBank ID: NM 002188). The mutant IL13.E13K.R109K was created by PCR with mutagenic primers based on the hIL13 cDNA sequence. The transmembrane and cytoplasmic domains were amplified by PCR from hCD3ζ cDNA clone obtained from ATCC (GenBank ID: BC025703). The human cytoplasmic CD28 chain, the hinge region of human CD8α, and an Ig heavy chain signal sequence (VHCAMP) were amplified by PCR from pMFG-CEA (18). Each product was digested with restriction enzymes, ligated, and amplified by PCR. Monomeric CAR was generated by mutating both Cys-29 of the CD8α hinge and Cys-2 of CD3 transmembrane to Ala using mutagenic primers. The assembled construct was sequenced then cut and ligated into *Bam*HI-*Not*I cleaved MFG retroviral expression vector.

Retrovirus production and genetic modification of primary human T cells

Retroviral supernatants were prepared and peripheral blood T cells activated and transduced as described previously (19). Human peripheral blood mononuclear cells (PBMC) were Ficoll-isolated from blood filter discards (Rhode Island Blood Center, Providence, RI) and then activated in the presence of OKT3 (50 ng/mL) and IL2 (300 U/mL) for 36 to 48 hours. Cultured cells were then "spinfected" by centrifugation with retrovirus-containing supernatants plus protamine in a retronectin-coated plate for 1 hour at room temperature. This step was repeated 2 more times in the next 24 hours and then transferred to fresh RPMI-1640 medium containing 10% FBS, antibiotics, and IL2 (300 IU/mL) with a 10- to 20-fold expansion over a period of 1 to 2 weeks. After 1 week in culture, cultures were more than 95% T cells, as used in the assays. Activated untransduced (UnTd) T cells from the same isolation were used as control group in all experiments.

Western blot

Transduced T cells (10^7) were coincubated overnight with tunicamycin, an inhibitor of *N*-linked glycosylation, and then processed to membrane fractions of protein using Mem-per Protein Extraction (Thermo-Fisher) per

manufacturer's instructions and analyzed as described previously (18).

Flow cytometric analysis

Flow cytometry used an LSR II instrument (Becton Dickinson) and FACSDiva software (Becton Dickinson). Phycoerythrin (PE)-conjugated antihuman IL13 antibody (Becton Dickinson) was used to detect CAR expression on transduced T cells. U251 and Thp-1 cell lines were analyzed with anti-human IL13Rα2 antibody (R&D Systems) with anti-mouse fluorescein isothiocyanate (FITC) secondary antibody (R&D Systems) or anti-human IL13Rα1 phycoerythrin (R&D Systems). In all cases, negative controls included isotype antibodies.

Cytotoxicity assay for redirected tumor cell killing

The cytolytic activity of T-cell effectors was determined by CytoTox-GloTM Cytotoxicity Assay (Promega). Effector cells were plated in 96-well plates at 37°C for 22 hours in triplicate at 5,000 per well with 10,000 U251 or HUVEC target cells [effector (E):target (T) = 0.5:1] or for 5 hours in triplicate at 50,000 per well with 10,000 target cells (E:T = 5:1).

Analysis of cytokine production

Untransduced (UnTd) activated T cells and CAR$^+$ T-cell effectors (2×10^5) were cocultured in 96-well plates with target cells (1×10^5) in duplicate in 200 µL of culture medium (E:T = 2:1). After 24 hours, supernatants were assayed for IL2 and IFNγ by ELISA (R&D Systems). The media in Fig. 3 were supplemented with IL2 that was subtracted as a background reading on control cultures without cell targets (ca. 200 pg/mL). Adjustment was then made for CAR$^+$ fractions (20%–24%) as necessary for construct comparisons. See Supplementary Material for detailed explanation of controls and data reduction to create this Figure. In Fig. 4, cytokine assays did not include IL2, yielding IL2 levels in unstimulated dTc and control UnTd T cells <10 pg/mL. In this figure, results with dTc were not adjusted for CAR$^+$ fraction (~30%).

Proliferation and expansion assays

Activated T-cell effectors (1×10^6) were cocultured with irradiated (7,000 rads) target cells (5×10^5) in 24-well plates in 1 mL of culture medium and supplemented with 5 IU/mL IL2 (E:T = 2:1). The T-cell cultures were restimulated on day 7 with fresh irradiated targets. Viable T cells were assayed by trypan blue exclusion. The starting and final CAR$^+$ fractions were assessed by flow cytometry.

Calculations of CAR$^+$ cell expansions

With a mixture of normal and CAR$^+$ T cells, an antigen-induced difference in the expansion rate of the modified cells is revealed in the net change in total cell numbers. The fold change of the dTc component from baseline (day 0) is given by $\gamma_2 = 1/f_1 [\gamma_3 - \gamma_1 (1 - f_1)]$, in which γ_1 is the fold

increase of cells in the control culture, γ_3 is the fold increase of total cells in the stimulated culture, and f_1 is the original fraction of CAR$^+$ cells in the mix. Using values of 13, 20, and 0.03, respectively, from Fig. 4C and D, a value of $\gamma_2 = 250$-fold increase in dTc is derived. Compared with the control expansion, there is $n = \gamma_2/\gamma_1 = 250/13 = 19$-fold greater expansion of the dTc over this time period due to stimulation. When considered in terms of growth rate constants (e.g., k in e^{kt}), the impact is seen as $k_2/k_1 = \log(\gamma_2)/\log(\gamma_1)$ in this formulation, with a $\log(250)/\log(13) = 2.1$-fold increase in the growth rate constant with antigen stimulation, comparable with values previously derived with CEA- and GD3-specific dTc (18, 20). For derivations, see Appendix.

We also consider the reverse method of inferring the impact of stimulation to increase dTc proliferation from the higher fraction of CAR$^+$ cells. The relative fold increase in dTc (γ_2/γ_1) is given as $n = [(1 - f_1)/f_1] [f_2/(1 - f_2)]$, in which f_1 and f_2 are the starting and ending CAR$^+$ fractions. When applied to data of Fig. 4D (subtracting backgrounds), $f_1 = 0.03$ and $f_2 = 0.38$, yielding an $n = 20$-fold relative expansion in dTc versus control over the assay period poststimulation, corroborating the above result ($n = 19$). This contrasts with a smaller, 12.7-fold change in percentage (3%–38%). The CAR$^+$ fraction changes more slowly than the fold increase in CAR$^+$ cells because the new CAR$^+$ cells increase the denominator as well as the numerator. For derivations, see Appendix. See also ref. 18.

Intracranial glioma model

Female nude rats, 125 to 175 grams (Charles River Laboratories), were anesthetized and the head shaved and prepared with alcohol and Prepodyne solution (West Penetone). A midline scalp incision was made, exposing the sagittal and coronal sutures. A 2-mm burr hole was made with an electric drill, centered 3 mm lateral to the sagittal suture and 5 mm posterior to the coronal suture, avoiding the sagittal sinus. Rats were then placed in a stereotactic frame (David Kopf), and 1×10^6 U251 glioblastoma cells suspended in 5 µL culture medium were injected over 3 minutes via a 26-gauge needle inserted to a depth of 3 mm at the center of the burr hole. Following the injection, the needle was left in place for 3 minutes to avoid tumor cell extrusion and then withdrawn and the incision closed with surgical staples. Experiments were carried out under protocols approved by the Animal Care and Use Committee of Johns Hopkins University.

In vivo efficacy study

Six days after tumor injection, the tumor-bearing rats were randomized into 3 groups for treatment with 5×10^6 dTc (32% modification; $n = 13$); or 5×10^6 UnTd activated T cells in 25 µL ($n = 12$) at the same tumor coordinates; or no treatment ($n = 6$). Rats were observed for systemic and neurologic toxicity and death was recorded. At day 120, the experiment was terminated and surviving rats were euthanized.

MRI

Two rats per group were selected at random for MRI at 1, 2, and 3 weeks following treatment, under isofluothane anesthesia. Multislice T2-weighted imaging with fast spin echo acquisition was acquired.

Brain histology and immunohistochemistry

Two rats per group selected at random were anesthetized with pentobarbital (100 mg/kg intraperitoneally) and perfused transcardially with 4% paraformaldehyde. Brain tissue was harvested, fixed in 10% formalin, blocked in paraffin, sectioned in a coronal plane in 5-μm sections, and stained with hematoxylin and eosin (H&E) and anti-CD3. Brain histology experiments were carried out by Johns Hopkins Medical Laboratories Reference Histology, and immunostaining conducted in the Roger Williams Medical Center Pathology Department.

Statistical analysis

Cytotoxicity and cytokine production results were expressed as mean $\pm$ SEM and analyzed using the Student t test. $P < 0.05$ was considered statistically significant. For *in vivo* efficacy, death was the primary endpoint. The distribution of the intervals until death was analyzed by the method of Kaplan and Meier.

Results

A central concern for any redirected cellular therapy is the specificity of the targets for tumorous versus normal expression of antigen on essential organs. The potency and accompanying potential for hazard of the dTc platform was graphically showed with the toxic death of the first patient treated with dTc expressing a CAR against Her2/neu, which has low expression in the lung, bowel, and heart tissues that were targeted (21). Accordingly, a major focus is rightly on the selectivity of the CAR for IL13Rα2, with distribution largely restricted to GBM, versus the normal IL13Rα1/IL4Rα that is expressed widely in the body.

Previous studies showed that substitutions at 2 sites (Lys-105 and Arg-109) in IL13 could enhance IL13 binding to IL13Rα2, whereas substitution at Glu-13 in IL13 could decrease IL13 binding to the IL4Rα component of the high-affinity IL13Rα1/IL4Rα receptor (15–17, 22, 23). Therefore, we designed a novel mutant IL13.E13K.R109K (Glu-13 and Arg-109 both changed to Lys) that we hypothesized would enhance selectivity for recognition of IL13Rα2 of GBMs.

In addition, we assessed a further change to improve the potency of the dTcs. The IL13Rα2 that is expressed on glioblastomas is monomeric in structure. We speculated that monomeric CARs interacting with this monomeric receptor might allow for a tighter clustering of CAR signaling domains for improved dTc signaling and activation. Alternatively, CARs already in dimeric form might better present cytoplasmic domains for cluster-initiated signaling, increasing domain concentrations locally.

To address these hypotheses, we planned monomeric (m) and dimeric (d) IL13 wild-type (Wt = IL13.CD28.ζ) and mutant (Mu = IL13.E13K.R109K.CD28.ζ) CARs comprising an extracellular wt or mutant IL13 molecule linked to intracellular signaling components from CD28 co-stimulatory molecule and the CD3ζ molecule. We incorporated CD28 signaling into the CAR as tumor cells do not typically express B7, the natural ligand for CD28. This second-generation CAR transmits TCR signal 1 and CD28 signal 2 to resist activation-induced T-cell death (AICD), providing prolonged antitumor effects (18, 24–27).

Creation of IL13.CD28.ζ designer T cells

To create the dimeric wild-type (dWt) IL13.CD28.ζ CAR, we adapted our prior MFG retroviral CD28.ζ vector (18) that supplies intracellular signaling components from the CD28 cytoplasmic domain and the CD3ζ domain in a colinear design (Fig. 1A). In place of the CD28 transmembrane and extracellular domain (ECD) of our prior constructs, we substituted a CD3ζ transmembrane domain to maintain CAR dimerization without an ECD; with CD28 transmembrane, the ECD is needed for dimerization to occur. This condensed format allowed us to study the impact of the presence or absence of an extracellular spacer on IL13 CAR expression and function.

Initial optimization studies compared the native IL13 leader with the canonical immunoglobulin heavy chain leader used in our other constructs (18, 20) and compared the CAR expression with the presence or absence of a CD8a hinge domain. OKT3-activated T cells from a healthy donor were transduced with the MFG vectors to generate functional IL13.CD28.ζ CAR$^+$ dTc. Expression was determined by staining with anti-IL13 antibody (Fig. 1B). These tests proved critical for optimal gene expression. The heavy chain leader was much superior to the native IL13 leader for surface expression. Furthermore, there was little surface staining without the hinge domain, suggesting poor surface transit for this CAR or steric hindrance in antibody binding due to the IL13-to-membrane juxtaposition. This format with heavy chain leader plus hinge spacer was used for all ensuing studies.

Next, we examined the possibility to create a monomeric CAR (Fig. 2A). For this, we mutated the cysteine to alanine (Cys → Ala) in the CD3ζ transmembrane and in the extracellular CD8α hinge region that maintain dimerization of the CAR. As the final variation, we created a mutant IL13 (IL13.E13K.R109K) that includes alterations to improve the reactivity against IL13Rα2$^+$ gliomas (R109K) while reducing attack against normal tissues bearing IL13Rα1/IL4Rα (E13K) (23). When the CARs were expressed, Western blotting on nonreducing gels confirmed monomeric (∼40 kDa) and dimeric (∼80 kDa) products (Fig. 2B). Allowing for differences in vector supernatant titers, all formats were equally well-expressed by fluorescence intensity of surface staining on flow cytometry (Fig. 2C).

Signaling is equivalent between monomeric and dimeric CARs but superior with mutant IL13 CARs

To select an agent for development, we tested the aforementioned hypotheses of action in a T-cell stimulation assay with IL2 secretion as read-out. Functional tests were

Figure 1. Construction of IL13 CAR. A, plasmid map of IL13-CAR.pMFG. The IL13.CD28.ζ CAR expression cassette was constructed and cloned into BamHI and NotI sites of the MFG retroviral expression vector plasmid. B, CARs with different signal sequences (IL13, immunoglobulin heavy chain), with and without CD8a hinge, were constructed. Efficacy of CAR expression on the transduced T cells was tested by flow cytometry, with percent positive listed in each panel.
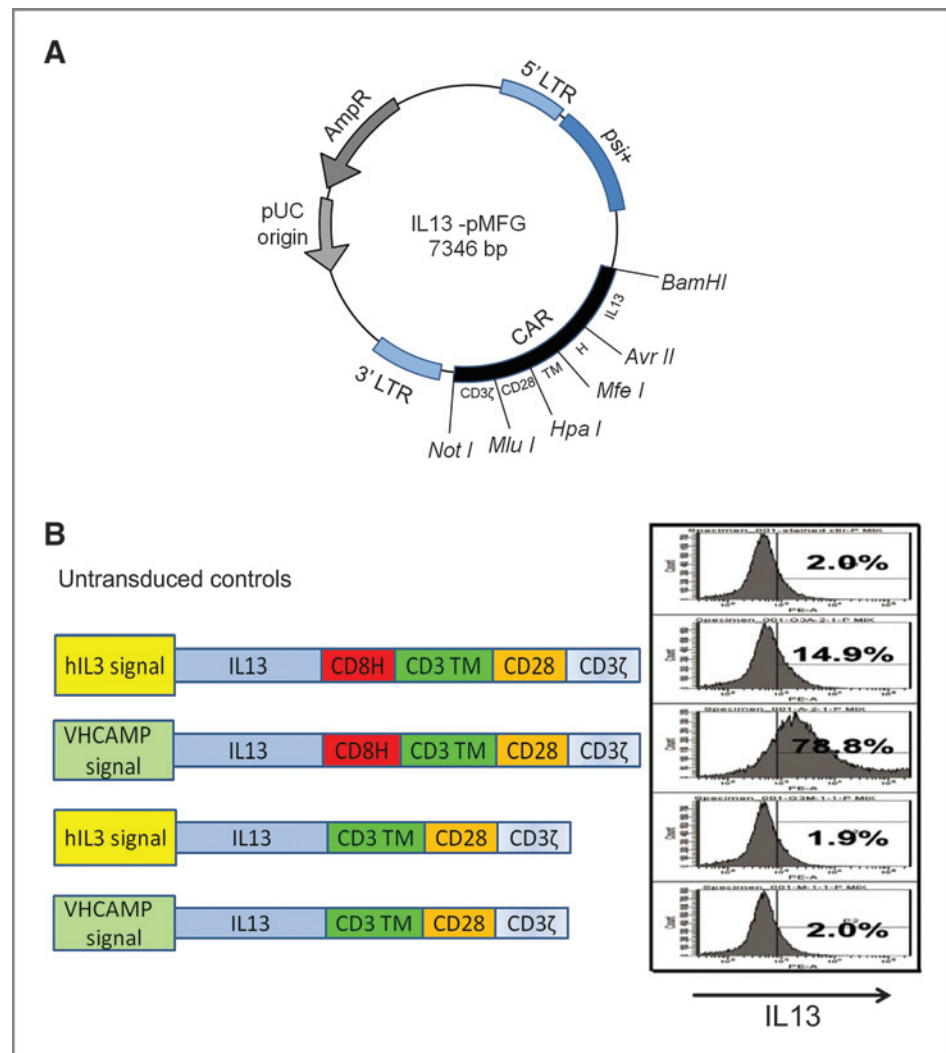
conducted with bulk modified T cells with a mixed population of CD4 and CD8 cells, reflecting current practice of clinical trials to infuse bulk modified T cells (28) that shift to inverted CD8/CD4 ratios on extended culture (20). Four configurations were tested for signaling potential by IL2 secretion: monomer wild-type (mWt) IL13 CAR, dimer wild-type (dWt) IL13 CAR, monomer mutant (mMu) IL13 CAR, and dimer mutant (dMu) IL13 CAR. Normal human T cells were modified to 20% to 25% and mixed 1:1 with stimulator target cells. Figure 3A shows IL13R profiles for stimulator cells used in this study: Thp-1 (IL13Rα1$^+$α2$^-$) and U251 (IL13Rα1$^-$α2$^+$). These represent the normal tissue and tumor-predominant IL13R, respectively.

IL2 secretion was abundant with all 4 of the constructs on both IL13R-positive cell lines (Fig. 3B; see Materials and Methods). Within each wt or mutant pair, the monomeric and dimeric CARs were equivalent, with no difference in signaling potential by this read-out, thus falsifying our hypothesis of a particular advantage to either the monomeric or dimeric format.

In contrast, the mutant IL13 displayed characteristics that supported our hypothesis of an improved selectivity of the mutant form, with heightened signaling on the IL13Rα2$^+$ cell targets and reduced signaling on the IL13Rα1$^+$ cells. Both of the IL13 wt CARs (monomer and dimer) had signaling activity against IL13R α1$^+$ and α2$^+$ targets, as expected, with the Thp-1 α1$^+$ targets more potently activating the IL13 CAR$^+$ T cells. In both of the mutant IL13 CARs, the signaling pattern was reversed, with the each dTc more potently activated by the U251 IL13R α2$^+$ target than by the α1$^+$ target. Thus, the mutant IL13 CARs were half as efficiently activated on IL13Rα1$^+$ Thp-1 cells and twice as efficiently activated on IL13Rα2$^+$ U251 cells, a 4-fold improvement in selectivity.

The preferred form for development was thus mutant IL13 CAR in either monomeric or dimeric format. For the remainder of the exposition, we present data on one form (monomer mutant, mMu IL13 CAR) that was taken forward from in vitro through in vivo testing.
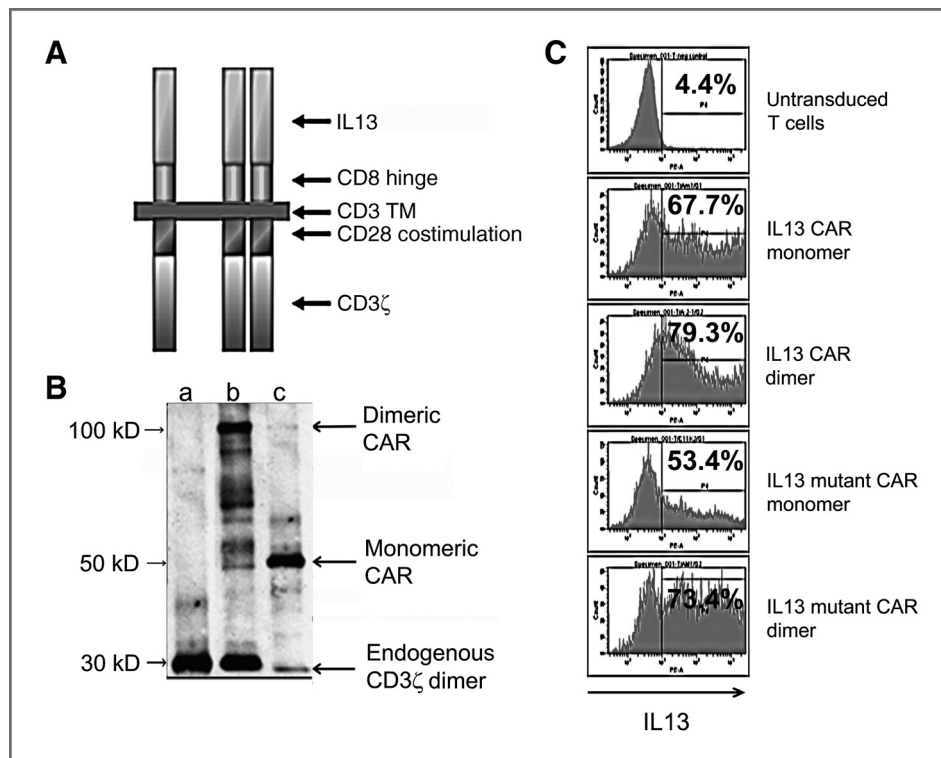
Figure 2. Expression of CAR on transduced T cells. A, graphic representation of the IL13 CAR showing monomeric and dimeric forms. B, Western blotting of CAR expression on membranes of transduced T cells, confirming monomer and dimer size bands versus control UnTd T cells. C, flow cytometric profiles of IL13 CAR expression on transduced T cells, with percent positive listed. Mean fluorescence intensity (MFI) of positive fractions was similarly high among all constructs (>10,000).

Functional characterization of monomer mutant (mMu) IL13.CD28.ζ designer T cells

Insertion of mMu IL13.CD28.ζ CAR into T cells genetically programs the resulting dTc to respond in an MHC-independent manner to IL13Rα2$^+$ glioblastoma cells with activation of T-cell effector functions. We assayed 3 mechanisms relevant to antitumor activity of IL13 dTc:cytotoxicity, cytokine production, and proliferation/resistance to AICD.

The single most critical feature of CAR$^+$ T cells for antitumor therapy is their antigen-directed killing capacity. We show that IL13 CAR$^+$ T cells recognize and kill IL13Rα2$^+$ glioblastoma cells (Fig. 4A). U251 cells were 60% killed in 5 hours with an E:T ratio of 5:1 that calculates to 1.25:1 dTc to targets, when allowing for fact that cells were 24% modified (Fig. 4A left). In a longer term assay with a lower E:T ratio of 0.5:1 (0.2:1 when adjusted for dTc fraction), 75% of targets were killed in 22 hours, showing multiple tumor cell (~3.5) killing per T cell in this interval (Fig. 4A, right). Activated UnTd T cells showed negligible killing under both conditions.

Cytokine production was assessed in terms of IL2 and IFNγ released by activated dTcs. IL2 is an essential growth factor for T-cell survival and proliferation, and secretion of IL2 and IFNγ has been correlated with tumor rejection (29–31). Previous studies showed that IL2 is produced principally by CD4 helper T cells and that IFNγ may be secreted by both CD4 and CD8 cells upon antigen engagement (31). Bulk unfractionated IL13 dTcs were cultured with target cells and supernatants assayed by ELISA. The IL13 dTcs produced IL2 (confirming results of Fig. 3) and IFNγ when cultured with IL13Rα2$^+$ U251 cells but not when cultured

with control IL13Rα$^-$ HUVEC cells (Fig. 4B). UnTd control T cells were negative for cytokine production on both targets.

A primary motivation for the second-generation format with CD28 costimulation was to avoid AICD and to foster dTc expansion on antigen contact. To test the potential for such expansion, we designed an experiment with coculture of T cells and IL13Ra2$^+$ targets, beginning with an intentionally low 3% dTc starting fraction and then monitoring total cell numbers and dTc fractions over time. Creation of dTcs involves a general activation of all T cells followed by vector transduction (Materials and Methods) that continues with a basal expansion of all T cells, modified and unmodified, over a month's period. In cocultures, IL13 dTcs proliferated 13-fold on Daudi cells over 2 weeks due to this basal expansion that increased to 20-fold on U251 cells (Fig. 4C). When adjusting for the initial 3% CAR$^+$ fraction, this increment in the dTc culture implied a 250-fold increase in the original CAR$^+$ T cells versus 13-fold in the unmodified cells. This corresponds to an $n = 19$-fold relative numeric increase (250/13) over the period and a doubling of the basal dTc expansion rate constant induced by tumor contact (i.e., 8.0 vs. 3.7 doublings; see Materials and Methods for calculations).

Proof of the selectively accelerated dTc growth is reflected in an enrichment of the dTc fraction by flow cytometry (Fig. 4D). Over 2 weeks, the 3% starting fraction of CAR$^+$ T cells (after background subtraction) increased to 38% (after background) on U251 targets but remained stable (4% after background) on antigen-negative Daudi cells. This enrichment calculates to an $n = 20$-fold relative expansion
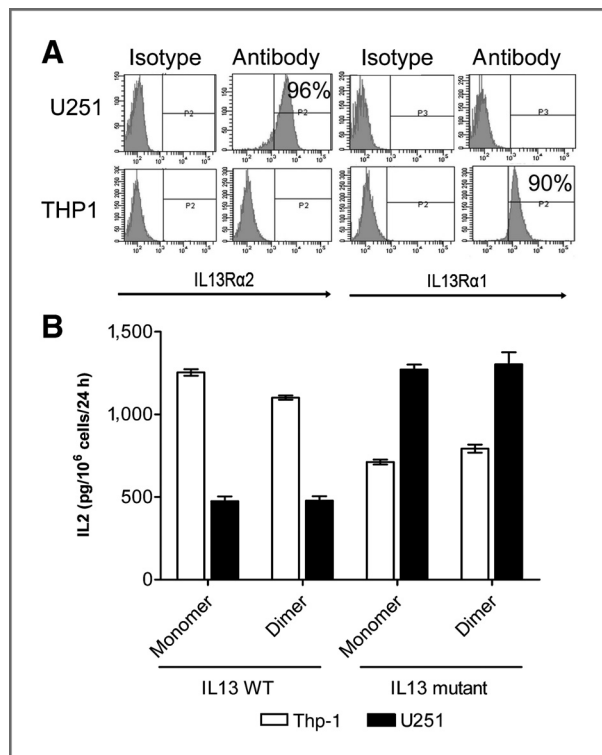
Figure 3. T-cell signaling via different CAR formats assessed by IL2 production by transduced T cells. A, flow cytometric profile of IL13Rα1 and IL13Rα2 expression on U251 glioma cells and Thp-1 cells. B, bar graph representing specific IL2 secretion by IL13 CAR transduced T cells upon coculturing with either IL13R (a1$^+$a2$^-$) Thp-1 cells (white bars) or IL13R (a1$^-$a2$^+$) U251 glioma cells (black bars) after background subtractions (Materials and Methods). IL2 levels are normalized to the percent of modified cells (range, 20%–24%) and expressed in pg/10^6 modified T cells/24 hours. Error bars represent SD from the mean of triplicate results.

of CAR$^+$ T cells on stimulation versus control, corroborating the above result ($n = 19$; see Materials and Methods for calculations).

A single intracranial injection of mMu IL13 designer T cells increases survival in a human glioma xenograft model

To determine the *in vivo* anti-glioma efficacy of locally injected mMu IL13 dTc, we used a human glioma xenograft model as described (32). A total of 1×10^6 IL13Rα2$^+$ U251 glioblastoma cells were stereo-tactically injected in the midbrain of 6- to 8-week-old nude rats. On day 6 after tumor implantation (study day 0), rats were randomized into 3 groups for treatment with 5×10^6 IL13 dTcs (32% modified, 80%–90% viability, $n = 13$); 5×10^6 UnTd activated T cells (>95% viability, $n = 12$); and no treatment ($n = 6$). T cells were injected to the tumor bed via the same stereotactic coordinates.

Two rats from each group were sacrificed at 1 week following T-cell injections for evaluation of tumor size and T-cell infiltration. H&E staining confirmed that IL13 dTc inhibited tumor growth: signs of tumor cell killing were found in rats treated with dTcs but not in control animals treated with UnTd-activated T cells (Fig. 5A). Adjacent sections were stained with anti-CD3 antibody to determine the persistence and trafficking of T cells within the glioma; tumors were infiltrated both with UnTd-activated T cells and with dTc but with the modified T cells in much greater abundance, suggesting improved dTc persistence or tumor-induced expansion (Fig. 5A).

Tumor volume change was followed over time by MRI in 2 rats per group (Fig. 5B). By MRI, no tumor was visualized in rats treated with dTc until 3 weeks following treatment. In contrast, tumors were apparent after 1 week and grew progressively to large size in animals that were either untreated or treated with UnTd-activated T cells (Fig. 5B).

Finally, this delayed growth of tumor on MRI was reflected in prolonged survival of the dTc treated animals. Rats that were untreated or treated with UnTd-activated T cells had median survivals of 35 days (range, 35–38; $n = 4$) and 40 days (range, 29–53; $n = 10$), respectively (Fig. 5C, Table 1). The 5-day improved survival in the T cell treatment group was statistically significant ($P < 0.03$; Table 1), compatible with a nonspecific LAK-type activity of activated T cells against tumor. In contrast, rats treated with IL3 dTcs had a median survival of 88 days (range, 47–120+; $n = 11$), with 28% surviving longer than 120 days ($P < 0.0001$ vs. UnTd-activated T cells; Table 1), indicating that the IL13 CAR confers important antitumor activity on the injected T cells.

Discussion

In this report, we describe the development and testing of designer T cells expressing a novel IL13Rα2-directed CAR, designated mMu IL13.CD28.ζ, as a promising therapeutic modality for GBM treatment. Following optimization tests, we obtained good expression of the CAR in normal human T cells, using an immunoglobulin heavy chain leader sequence, and interposing a flexible hinge between the IL13 cytokine and the membrane. The immunoglobulin heavy chain leader was superior to the native IL13 leader, and there was little surface CAR staining without the hinge domain. It was not distinguished whether the hinge improved surface transit or overcame a steric factor caused by membrane proximity that otherwise hampered access of antibody to its IL13 binding epitope.

The introduction of mutations in the IL13 domain improved the selectivity of the CAR for IL13Rα2 on tumor versus the IL13Rα1/IL4Rα that is expressed systemically. The R109K mutation has been shown to improve the affinity of IL13 for the IL13Rα2, and the E13K mutation was shown to decrease affinity for the widespread IL13Rα1/IL4Rα (17, 22). By putting these mutations together, we hoped to increase the potency of the IL13 dTcs against GBM targets while decreasing the activity against the normal tissue IL13Rα1/IL4Rα. With IL2 response as a signaling read-out, that increase was 2-fold against IL13Rα2$^+$ cells and the decrease was 2-fold against IL13Rα1$^+$ cells, for a 4-fold swing in activity. This led to selection of the mutant for further development. Similar comparisons of activity in monomeric or dimeric formats showed no differences, and a monomeric mutated form was applied in further studies.
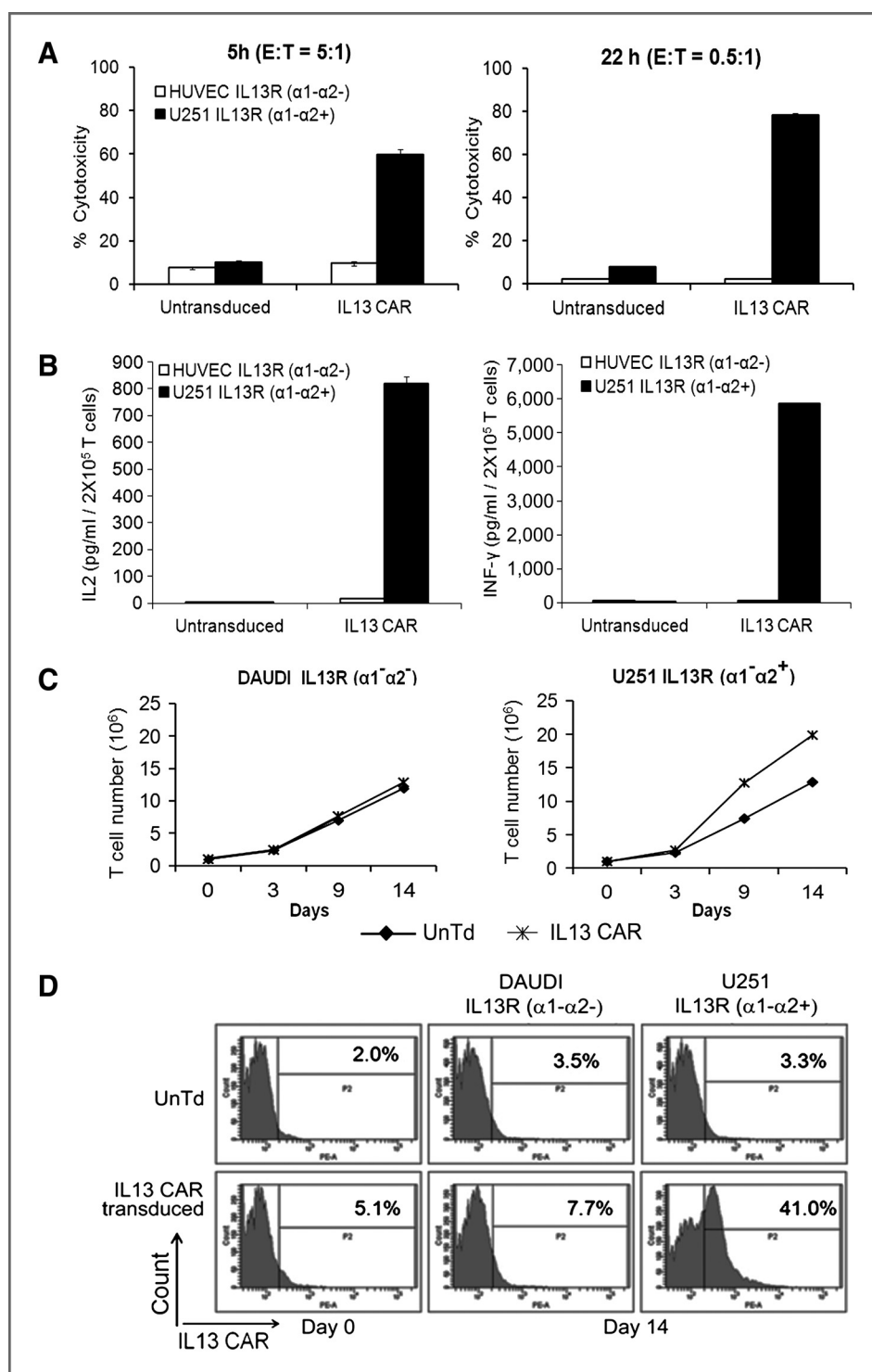
Figure 4. Functional characterization of IL13 CAR T cells. A, cytotoxic effects of IL13 CAR transduced versus untransduced T cells on U251 glioma cells (black bars) or control HUVEC cells (white bars). Left, cytotoxicity after 5 hours of co-culture with an E:T ratio of 5:1. Right, cytotoxicity after 22 hours of coculture with E:T ratio of 0.5:1. Error bars represent SEM from the mean of triplicate results. B, cytokine secretion by IL13 CAR transduced or untransduced T cells upon coculture with U251 glioma cells (black bars) or control HUVEC cells (white bars). Left, IL2; right, IFNγ. Cytokine levels expressed as pg/10^6 total T cells/24 hours, uncorrected for modified fraction (30%). Error bars represent SEM from the mean of triplicate results. C, dTc cell proliferation upon coculturing 1:1 with control Daudi cells (left) and U251 glioma cells (right) on days 0, 3, 9, and 14 and cell counts assayed (◆; UnTd T cells; Ж, IL13-CAR T cells). D, enrichment of IL13 CAR T cells upon coculture with stimulators. T-cell expansions in C with either U251 glioma cells or control Daudi cells were assayed by flow on day 0 and day 14. Top, untransduced (UnTd) T cells; bottom, IL13 CAR transduced T cells. The x-axis represents IL13 CAR expression, whereas y-axis represents cell count in the histogram plots.

These IL13 dTcs showed levels of cytokine production, tumor cell killing, and tumor-dependent T-cell expansion compatible with results seen in our other second-generation dTcs (18, 20). A single intracranial tumor injection of these IL13 zetakine/dTc into tumor-bearing rats resulted in a marked increase in survival in a human glioma xenograft model, including 28% long-term survivors who potentially represent cures. These survival benefits paralleled a heightened persistence and/or expansion of dTc in the tumor bed that in turn correlated with the *in vitro* studies showing that tumor induces selective expansion or persistence of the modified cells.

The quantitative benefit of the mutations in terms of signaling merits discussion. Considering the normal

Figure 5. Successful suppression of human glioma xenografts by IL13 CAR^{+} T cells. Rats with 6-day established U251 glioblastoma tumors were randomized into 3 groups for treatment on day 0: (i) CAR^{+} T cells, (ii) UnTd T cells, and (iii) no treatment. A, representative brain histology. At day 7, after T-cell injection, progressing and regressing tumors were assessed by H&E (a and b) and anti-CD3 mAb staining (c–e); (a) UnTd: A 4-mm tumor is shown; (b) dTc: An indistinct band of tumor with a 5-mm zone of associated inflammation. Immunostaining: Anti-CD3 immunostaining showed increased T cells in the dTc treated tumors (d and e) versus tumors treated with UnTd T cells (c). B, T2-weighted MRI of tumor-bearing animals at indicated times following treatment. For each rat, 3 acquired slices are displayed at each time point to span the tumor zone. No visual tumor (open arrow) was observed in animals treated with CAR^{+} T cells. In contrast, large tumors (solid arrow) were observed in control group animals that grew progressively. C, Kaplan–Meier progression-free survival.
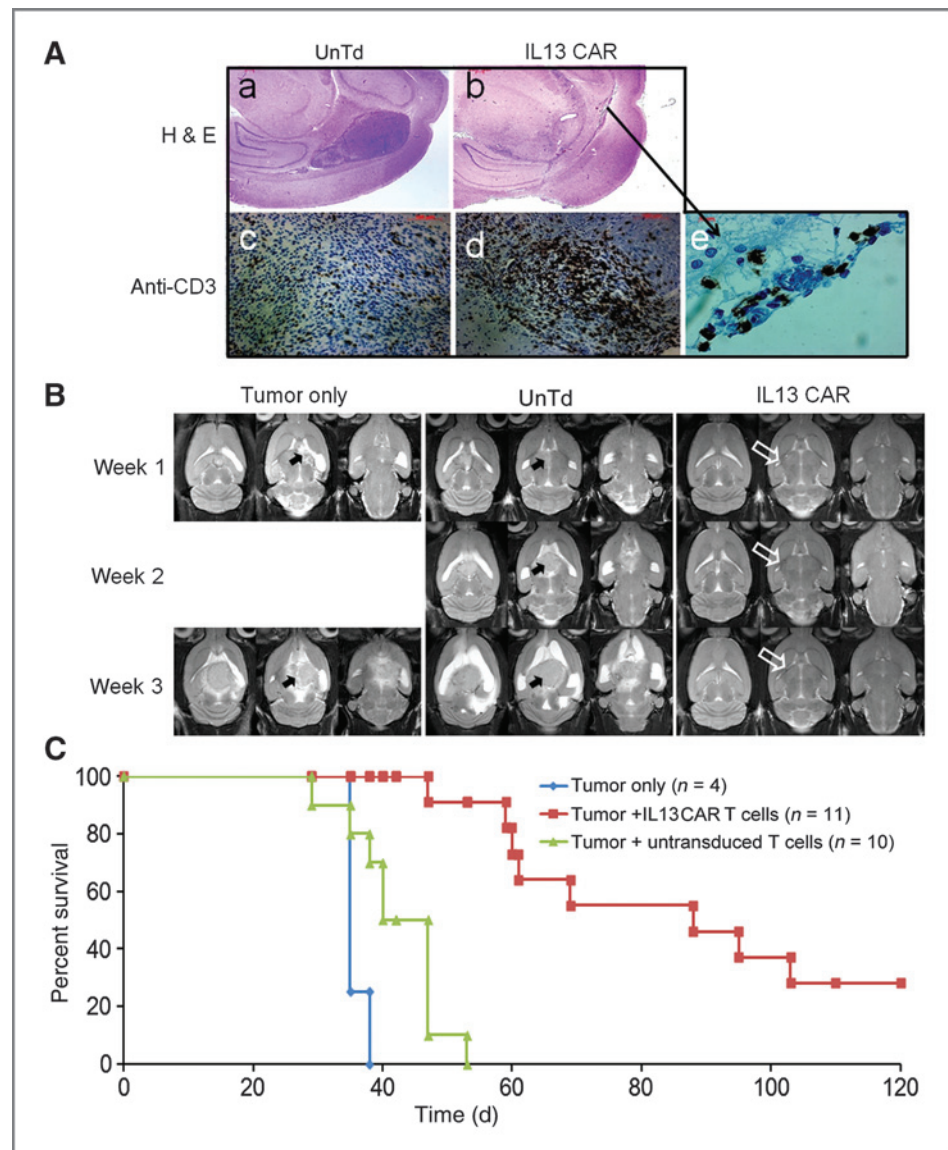
receptor interactions first, if we take as nominal the IL13 K_d for the widespread IL13Rα1/IL4Rα as 0.1 nmol/L, and then eliminate the binding to IL4Rα with the E13 mutation, we are still left with binding of IL13 by IL13Rα1 with a 10 nmol/L K_d (13-15). As presented, this is a 100-fold swing in affinity *away from* the IL13Rα1/IL4Rα receptor, yet the IL13 dTcs on control α1[+] Thp-1 cells show only a 2-fold reduc-

tion in activation by our measure. Similarly, the R109K mutation is said to *increase* IL13 affinity for the glioma-associated IL12Rα2 by nearly 30-fold (17), yet we observe only a 2-fold benefit in dTc activation on α2[+] U251 GBM cells. The discrepancies are likely to lie in the multivalent nature of the CAR interaction with the antigen on the tumor cell that may obscure differences that are apparent with

Table 1. *In vivo* efficacy of IL13 dTc

Group	Median survival (range), d	Long-term survivors (>120 d), %	P
Tumor, no treatment (n = 4)	35 (35–38)	0	<0.03 vs. no treatment
Tumor + UnTd T cells (n = 10)	40 (29–53)	0	<0.0001 vs. no treatment;
Tumor + IL13 dTc (n = 11)	88 (47–120+)	28	<0.0001 vs. UnTd T cells

monovalent ligands (e.g., IL13 immunotoxin). It was previously shown that CAR or TCR affinity above a certain threshold ($\sim$10 nmol/L K_d) does not increase T-cell activation by cellular antigens (33), and below this threshold, that activation is achieved with a product of receptors times affinity, in a mass action type of formulation (34). Furthermore, it may be noted that even 10 nmol/L K_d [10^8 (mol/L)$^{-1}$ K_a] still greatly exceeds typical TCR affinities [10^5–10^7 (mol/L)$^{-1}$ K_a]. We should therefore not be surprised that the residual binding activity for the normal IL13Rα1 in our mutant IL13 retains substantial T-cell stimulation potency.

These data merit comparison with the results of Kahlon and colleagues (6) who coined the term zetakine and were the first to prepare an IL13 CAR. In their studies, they used a first-generation version of the IL13 dTc versus our second-generation version. They used a single E13Y mutant versus our double mutant that used E13K with R109K. The E13Y was selected to reduce affinity for the normal tissue IL13Rα1/IL4Rα, like the E13K that we use, whereas we add the second mutation in an attempt to increase CAR affinity for the GBM receptor that could improve reactivity against tumor with lesser amounts of antigen. They, like we, also had a hinge spacer, but one (Fc) which generates solely a dimeric format (which we show is equivalent to monomeric). Finally, they applied plasmid transfer for limited duration expression instead of retroviral transfer, as in our case, that provides stable CAR expression.

In terms of cytotoxicity and IFNγ production, our data parallel that of Kahlon and colleagues (6). We show abundant IL2 production as expected for second-generation that would not be expected with their earlier first-generation design, yet they show good production as well. Interestingly, they explained their result by the presence of ligands on the target cell lines that interact with costimulatory molecule NKG2D on the T cells to provide Signal 2. They show ^{3}H-thymidine incorporation in their dTcs on antigen contact, but this is not quantitated in terms of actual cell number increases, and repair synthesis associated with apoptosis has been noted to incorporate thymidine (35); in any case, the proliferative response, if any, could have benefited from costimulation in the same fashion as did IL2 secretion. In the end, Kahlon and colleagues showed excellent activity in animal models analogous to ours, with intracranial injection of established tumors, including complete tumor suppressions. Potential advantages in our product are the double mutant, in which the higher affinity of our second mutation is shown to improve signaling, which may be important for attacking low antigen–expressing tumors; the incorporation of costimulation, which may be critical for activity in particular tumors lacking costimulatory ligands; and the retroviral delivery, which yields dTc with permanent modification, thus able to maintain antitumor surveillance for prolonged periods.

The results reported here are encouraging for human application against recurrent or resected malignant gliomas, with the demonstration of sufficient power to eliminate residual tumor by intratumoral injections. Yet, some discussion is warranted about the selectivity of our CAR for the intended tumor target in such clinical applications. At some level, the improvement in selectivity we have shown may be deemed an advantage. However, the recognition by dTcs with the mutated CAR against normal tissue IL13Rα1 remains substantial, and no presumption of safety for normal tissues can be inferred. The consequences of an error in that assumption have the potential to be fatal, depending upon how the dTcs are applied (21, 36), and we would accordingly not propose to apply this construct systemically. An alternative, however, may be to recapitulate our model of intra-tumoral (or intracavitary) brain delivery of IL13 dTc in a human application, potentially arming the dTcs with a suicide gene (37) to eliminate persisting dTcs if leaking out of the tumor site to cause systemic toxicity. In this regard, the lack of toxicity in the rats from the IL13 dTc injection is mildly reassuring for a local delivery, in as much as human IL13 and IL13-based dTcs will react with the rodent IL13Rα1 ortholog (Raj Puri, personal communication). Alternatively, still-more-selective mutations or antibodies could be developed for a safe human clinical application; ideally, one would have a recognition domain in the CAR that is absolute for the α2 receptor with no α1 reactivity whatsoever.

Appendix

Derivations:

I. We model growth of a mixed culture of CAR$^+$ and CAR$^-$ T cells as the sum of the independent growths of the 2 cell types, adjusted by the starting proportion of each cell type:

$$\gamma_3 = (1 - f_1)\, \gamma_1 + f_1 \gamma_2 \qquad \text{(A)}$$

In this, γ_1 = fold expansion of CAR$^-$ cells (the growth rate of the unstimulated culture), γ_2 = fold expansion of CAR$^+$ cells upon stimulation, γ_3 = fold expansion of the mixed culture, f_1 = starting fraction of dTc in mixed culture.

On rearrangement to solve for γ_2, Eq. A yields

$$\gamma_2 = 1/f_1 \left[\gamma_3 - (1 - f_1)\gamma_1 \right] \qquad \text{(B)}$$

The fold change in growth for the dTc on antigen stimulation is given as:

$$n = \gamma_2/\gamma_1 \qquad \text{(C)}$$

II. The ratio of growth rate constants is derived as follows. The relative growth of the 2 cell fractions is given by $\gamma_1 = e^{k_1 t}$ and $\gamma_2 = e^{k_2 t}$. The log of both sides yields $\log \gamma_1 = k_1 t$ and $\log \gamma_2 = k_2 t$. Dividing the second equation by the first yields the ratio of rate constants:

$$k_2/k_1 = \log \gamma_2 / \log \gamma_1 \qquad \text{(D)}$$

III. The fold change in growth for dTc upon stimulation [Eq. C] can also be inferred from the fractions of dTc in the culture at the start (f_1, as above) and at the end (f_2) of the experiment. $f_1 \gamma_2$ is the expansion of dTc in the mix in Eq. A,

in which γ_3 is the total expansion of all cells. Therefore, the new fraction is given by:

$$f_2 = \frac{f_1 \gamma_2}{\gamma_3} = \frac{f_1 \gamma_2}{(1-f_1)\gamma_1 + f_1 \gamma_2} \quad (E)$$

Rearrangement of Eq. E yields the ratio of dTc to control expansions, analogous to Eq. C:

$$n = \gamma_2/\gamma_1 = \frac{1-f_1}{f_1} \cdot \frac{f_2}{1-f_2} \quad (F)$$

Disclosure of Potential Conflicts of Interest

No potential conflicts of interest were disclosed.

Authors' Contributions

Conception and design: S. Kong, S. Sengupta, A.J. Bais, Q. Ma, R.P. Junghans, P. Sampath
Development of methodology: S. Kong, S. Sengupta, B. Tyler, Q. Ma, A. Sahin, R.P. Junghans, P. Sampath
Acquisition of data (provided animals, acquired and managed patients, provided facilities, etc.): S. Kong, S. Sengupta, B. Tyler, J. Zhou, B. Carter

Analysis and interpretation of data (e.g., statistical analysis, biostatistics, computational analysis): S. Kong, S. Sengupta, B. Tyler, J. Zhou, H. Brem, R.P. Junghans, P. Sampath
Writing, review, and/or revision of the manuscript: S. Kong, S. Sengupta, J. Zhou, A. Sahin, B.S. Carter, H. Brem, R.P. Junghans, P. Sampath
Administrative, technical, or material support (i.e., reporting or organizing data, constructing databases): S. Kong, A.J. Bais, Q. Ma
Study supervision: S. Kong, S. Sengupta, Q. Ma, H. Brem, R.P. Junghans, P. Sampath
Pathologic analysis of tumor tissue including interpretation of tumor histology and immunohistochemical staining of T cells: S. Doucette

References

1. DeAngelis LM. Brain tumors. N Engl J Med 2001;344:114–23.
2. Chang SM, Parney IF, Huang W, Anderson FAJ, Asher AL, Bernstein M, et al. Glioma outcomes project investigators patterns of care for adults with newly diagnosed malignant glioma. JAMA 2005;293:2469–70.
3. Attenello FJ, Mukherjee D, Datoo G, McGirt MJ, Bohan E, Weingart JD, et al. BCNU wafer in surgical treatment of glioma. Ann Surg Oncol 2008;15:2887–93.
4. Sadelain M, Brentjens R, Rivière I. The promise and potential pitfalls of chimeric antigen receptors. Curr Opin Immunol 2009;20:205–23.
5. Facoetti A, Nano R, Zelini P, Morbini P, Benericetti E, Ceroni M, et al. Human leukocyte antigen and antigen processing machinery component defects in astrocytic tumors. Clin Cancer Res 2005;11:8304–11.
6. Kahlon KS, Brown C, Cooper LN, Raubitschek A, Forman SJ, Jensen MC. Specific recognition and killing of glioblastoma multiforme by interleukin 13-zetakine redirected cytolytic T cells. Cancer Res 2004;64:9160–6.
7. Yaghoubi SS, Jensen MC, Satyamurthy N, Budhiraja S, Paik D, Czernin J, et al. Noninvasive detection of therapeutic cytolytic T cells with 18F-FHBG PET in a patient with glioma. Nat Clin Pract Oncol 2009;6:53–8.
8. Bullain SS, Sahin A, Szentirmai O, Sanchez C, Lin N, Baratta E, et al. Genetically engineered T cells to target EGFRvIII expressing glioblastoma. J Neurooncol 2009;94:373–82.
9. Debinski W, Gibo DM, Hulet SW, Connor JR, Gillespie GY. Receptor for interleukin 13 is a marker and therapeutic target for human high-grade gliomas. Clin Cancer Res 1999;5:985–90.
10. Mintz A, Gibo DM, Slagle-Webb B, Christensen ND, Debinski W. IL13Ralphα2 is a glioma-restricted receptor for interleukin-13. Neoplasia 2004;4:388–99.
11. Husain SR, Puri RK. Interleukin-13 receptor-directed cytotoxin for malignant glioma therapy: from bench to bedside. J Neurooncol 2003;65:37–48.
12. Kawakami M, Leland P, Kawakami K, Puri RK. Mutation and functional analysis of IL-13 receptors in human malignant glioma cells. Oncol Res 2001;12:459–67.
13. Hilton DJ, Zhang JG, Metcalf D, Alexander WS, Nicola NA, Willson TA. Cloning and characterization of a binding subunit of the interleukin 13 receptor that is also a component of the interleukin 4 receptor. Proc Natl Acad Sci U S A 1996;9:497–501.
14. Aman MJ, Tayebi N, Obiri NI, Puri RK, Modi WS, Leonard WJ. cDNA cloning and characterization of the human interleukin 13 receptor alpha chain. J Biol Chem 1996;271:29265–70.
15. LaPorte SL, Juo ZS, Vaclavikova J, Colf LA, Qi X, Heller NM, et al. Molecular and structural basis of cytokine receptor pleiotropy in the interleukin-4/13 system. Cell 2008;132:259–72.
16. Oshima Y, Puri R. Characterization of a powerful high affinity antagonist that inhibits biological activities of human interleukin 13. J Biol Chem 2001;7:15185–91.
17. Madhankumar AB, Mintz A, Debinski W. Interleukin-13 mutants of enhanced avidity toward the glioma-associated receptor, IL13Ralphα2. Neoplasia 2004;6:15–22.
18. Emtage PC, Lo AS, Gomes EM, Liu DL, Gonzalo-Daganzo RM, Junghans RP. Second-generation anti-carcinoembryonic antigen designer T cells resist activation-induced cell death, proliferate on tumor contact, secrete cytokines, and exhibit superior antitumor activity *in vivo*: a preclinical evaluation. Clin Cancer Res 2008;14:8112–22.
19. Beaudoin EL, Bais AJ, Junghans RP. Sorting vector producer cells for high transgene expression increases retroviral titer. J Virol Methods 2008;148:253–9.
20. Lo AS, Ma Q, Liu DL, Junghans RP. Anti-GD3 chimeric sFv-CD28/T cell receptor zeta designer T cells for treatment of metastatic melanoma and other neuroectodermal tumors. Clin Cancer Res 2010;16:2769–80.
21. Morgan RA, Dudley ME, Wunderlich JR, Hughes MS, Yang JC, Sherry RM, et al. Cancer regression in patients after transfer of genetically engineered lymphocytes. Science 2006;314:126–9.
22. Arima K, Sato K, Tanaka G, Kanaji S, Terada T, Honjo E, et al. Characterization of the interaction between interleukin-13 and interleukin-13 receptors. J Biol Chem 2005;280:24915–22.
23. Debinski W, Gibo DM, Obiri NI, Kealiher A, Puri RK. Novel anti−brain tumor cytotoxins specific for cancer cells. Nat Biotechnol 1998;16:416–49.
24. Harding CV, Unanue ER. Quantitation of antigen-presenting cell MHC class II/peptide complexes necessary for T cell stimulation. Nature 1990;346:574–6.
25. Viola A, Schroeder S, Sakakibara Y, Lanzavecchia A. T lymphocyte costimulation mediated by reorganization of membrane microdomains. Science 1999;283:680–2.
26. Moss WC, Irvine DJ, Davis MM, Krummel MF. Quantifying signaling-induced reorientation of T cell receptors during immunological synapse formation. Proc Natl Acad Sci U S A 2002;99:15024–9.

27. Finney HM, Lawson ADG, Bebbington CR, Weir ANC. Chimeric receptors providing both primary and costimulatory signaling in T cells from a single gene product. J Immunol 1998;161:2791–7.

28. Ma QZ, Gonzalo-Daganzo R, Junghans RP. Genetically engineered T cells as adoptive immunotherapy of cancer. In:Giaccone R, Schlinsky R, Sondel P, editors. Cancer chemotherapy and biological response modifiers, Annual 20. Oxford, England: Elsevier Science; 2002. p. 319–45.

29. Nakajima C, Uekusa Y, Iwasaki M, Yamaguchi N, Mukai T, Gao PM, et al. A role of interferon-y (IFN-y) in tumor immunity: T cells with the capacity to reject tumor cells are generated but fail to migrate to tumor sites in IFN-y-deficient mice. Cancer Res 2001;61:3399–405.

30. Haynes NM, Trapani JA, Teng MW, Jackson JT, Cerruti L, Jane SM, et al. Single-chain antigen recognition receptors that costimulate potent rejection of established experimental tumors. Blood 2002;100:3155–63.

31. Moeller M, Haynes NM, Kershaw MH, Jackson JT, Teng MW, Street SE, et al. Adoptive transfer of gene-engineered CD4+ helper T cells induces potent primary and secondary tumor rejection. Blood 2005;106:2995–3003.

32. Sampath P, Hanes J, DiMeco F, Tyler BM, Brat D, Pardoll DM, et al. Paracrine immunotherapy with interleukin-2 and local chemotherapy is synergistic in the treatment of experimental brain tumors. Cancer Res 1999;59:2107–14.

33. Chmielewski M, Hombach AA, Abken H. CD28 cosignalling does not affect the activation threshold in a chimeric antigen receptor-redirected T-cell attack. Gene Ther 2011;18:62–72.

34. Sykulev Y, Cohen RJ, Eisen HN. The law of mass action governs antigen-stimulated cytolytic activity of CD8+ cytotoxic T lymphocytes. Proc Natl Acad Sci U S A 1995;92:11990–2.

35. Sperling AI, Auger JA, Ehst BD, Rulifson IC, Thompson CB, Bluestone JA. Cd28/B7 interactions deliver a unique signal to naïve T cells that regulates cell survival but not early proliferation. J Immunol 1996;157:3909–17.

36. Junghans RP. Is it safer CARs that we need, or safer rules of the road? Mol Ther 2010;18:1742–3.

37. Di Stasi A, Tey SK, Dotti G, Fujita Y, Kennedy-Nasser A, Martinez C, et al. Inducible apoptosis as a safety switch for adoptive cell therapy. N Engl J Med 2011;365:1673–83.